

Dosimetry for Fractionated ^{131}I -mIBG Therapies in Patients with Primary Resistant High-Risk Neuroblastoma: Preliminary Results

Susan E. Buckley,¹ Frank H. Saran,¹ Mark N. Gaze,² Sarah Chittenden,¹ Mike Partridge,^{1,3} Donna Lancaster,¹ Andrew Pearson,³ and Glenn D. Flux^{1,3}

¹Royal Marsden NHS Foundation Trust, Sutton, Surrey, United Kingdom

²University College London Hospitals NHS Foundation Trust, London, United Kingdom

³Institute of Cancer Research, Sutton, Surrey, United Kingdom

ABSTRACT

This paper describes the development of a protocol for SPECT-based tumor dosimetry for ^{131}I -mIBG therapy patients with high-risk neuroblastoma. The treatment aims to deliver a whole-body dose of 4 Gy in two fractions. Whole-body retention measurements taken during the first fraction are used to guide the second therapy administration. The tumor dose from 3 patients was assessed by acquiring a minimum of three SPECT scans. Dead-time and triple-energy window scatter corrections were applied. The images were reconstructed using filtered backprojection with a Chang attenuation correction, and a phantom-based calibration factor was used to convert to activity. A monoexponential fit was made to the data, and instantaneous uptake was assumed. Tumor absorbed-dose ratios were used to analyze inpatient variations, and absolute tumor dosimetry was used to assess interpatient variation. The whole-body dose administered ranged from (3.7 ± 0.1) Gy to (3.9 ± 0.3) Gy. This method is more accurate than a weight-based administration method. Despite this, a variation in absorbed tumor dose of 10–103 Gy was observed. All repeat doses were in the same order of magnitude, although 2 patients received a lower tumor dose per MBq from the second therapy owing to a shorter biological half-life. The tumor dosimetry protocol was simple to apply and reproducible, but the errors in image quantitation need to be evaluated.

Key words: neuroblastoma, ^{131}I -mIBG, radionuclide therapy, dosimetry

INTRODUCTION

Neuroblastoma is a tumor of the autonomic nervous system, which, most commonly, arises in the adrenal gland. It typically presents in young children, with 96% occurring in patients less than

10 years old.¹ The prognosis of neuroblastoma is highly variable depending on age at diagnosis, stage of the disease, and tumor biology. The long-term survival for high-risk disease is less than 40%.² High risk is defined as neuroblastoma occurring in children over 1 year at diagnosis that have an amplification of the MYCN oncogene or distant metastases.³ Traditional treatment for these patients includes dose-intense induction chemotherapy, surgery, and high-dose chemotherapy. New and improved therapeutic strategies are needed to improve response rates in those

Address reprint requests to: Susan Buckley, Physics Department, Royal Marsden NHS Foundation Trust; Sutton, Surrey, SM2 5PT, UK; Tel.: +44-20-86613715; Fax: +44-20-86433812.

E-mail: Susan.buckley@icr.ac.uk

who do not respond adequately to induction chemotherapy to proceed to potentially curative therapy, and also for those who relapse after completion of treatment for whom, at the moment, there is no realistic prospect of a cure.

Metaiodobenzylguanidine (mIBG) is taken up by cells of the sympathetic nervous system (including tumors, such as neuroblastoma, which have been derived from them) by an active transport process involving the noradrenaline transporter molecule. When labeled with ^{131}I it has commonly been used for palliative therapy in heavily pretreated patients.^{2,4,5} However, an optimized treatment regimen, which might potentially contribute to a cure, has yet to be assessed in large-scale clinical trials.

Topotecan is a topoisomerase I inhibitor, which has been shown to act as a radiosensitizer and potentiate the effect of ^{131}I -mIBG when the two drugs are administered simultaneously, in both *in vitro* and *in vivo* experimental models.⁶ Theoretically, the benefit of ^{131}I -mIBG treatment could be enhanced by dose escalation and combination with topotecan.

One of the recently proposed treatment strategies uses a combination of high-dose ^{131}I -mIBG and topotecan.⁷ This schedule is myeloablative (as both ^{131}I -mIBG and topotecan contribute to hematological toxicity) and requires hemopoietic stem cell support to overcome myelosuppression, which is the dose-limiting toxicity. This protocol aims to give a total whole-body radiation-absorbed dose of 4 Gy. It does this through dosimetry-guided administrations given 2 weeks apart. The hope was to increase the administered activity of ^{131}I -mIBG beyond conventional levels while controlling toxicity by achieving, but not significantly exceeding, a desired whole-body absorbed radiation dose of 4 Gy.

It is supposed that the administration of a higher activity of ^{131}I -mIBG will result in a higher tumor radiation-absorbed dose, and a greater likelihood of response. However, partly

owing to difficulties associated with image quantitation in targeted radionuclide therapy (TRT), the relationship between administered activity, tumor-absorbed dose, and response remains unknown. If evidence of a tumor dose response relationship can be found, dose escalation studies to establish second-line toxicities will be possible to further optimize patient treatment.

Previous research introduced the concept of absorbed-dose ratios to compare the tumor dose received in the same patient during repeated therapies to reduce the errors that are traditionally associated with image quantitation.⁸ This study aimed to extend this work to compare the tumor doses received by the 3 patients in whom detailed dosimetry data were available. We also assessed the accuracy of administering the treatment based on whole-body dosimetry and suggest a simple protocol that could be used to assess the radiation-absorbed tumor dose reproducibly at different centers, enabling tumor dosimetry to be performed in a multicenter trial for this treatment regimen.

MATERIALS AND METHODS

Patients

Three (3) patients, 2 girls and 1 boy, whose ages ranged from 3 to 5 years, were treated with this schedule. Patient 1 had multiple relapsed stage 4 disease, patient 2 had relapsed stage 3 disease, and patient 3 had stage 4 disease, which had not responded to induction chemotherapy. All 3 patients had primary tumors located in the abdomen, and patients 1 and 3 also had skeletal metastases in the long bones. They were all treated compassionately with palliative intent. The patient data are summarized in Table 1.

Whole-Body Dosimetry

The therapy for this study was administered according to the schedule shown in Table 2 and has

Table 1. Patient Data

	<i>Age at time of treatment (years)</i>	<i>Patient weight (kg)</i>	<i>Administered activity—therapy 1 (MBq)</i>	<i>Administered activity—therapy 2 (MBq)</i>
Patient 1	4.8	15.4	6574	12,458
Patient 2	3.8	12.5	6869	4892
Patient 3	4.5	17.5	6893	9363

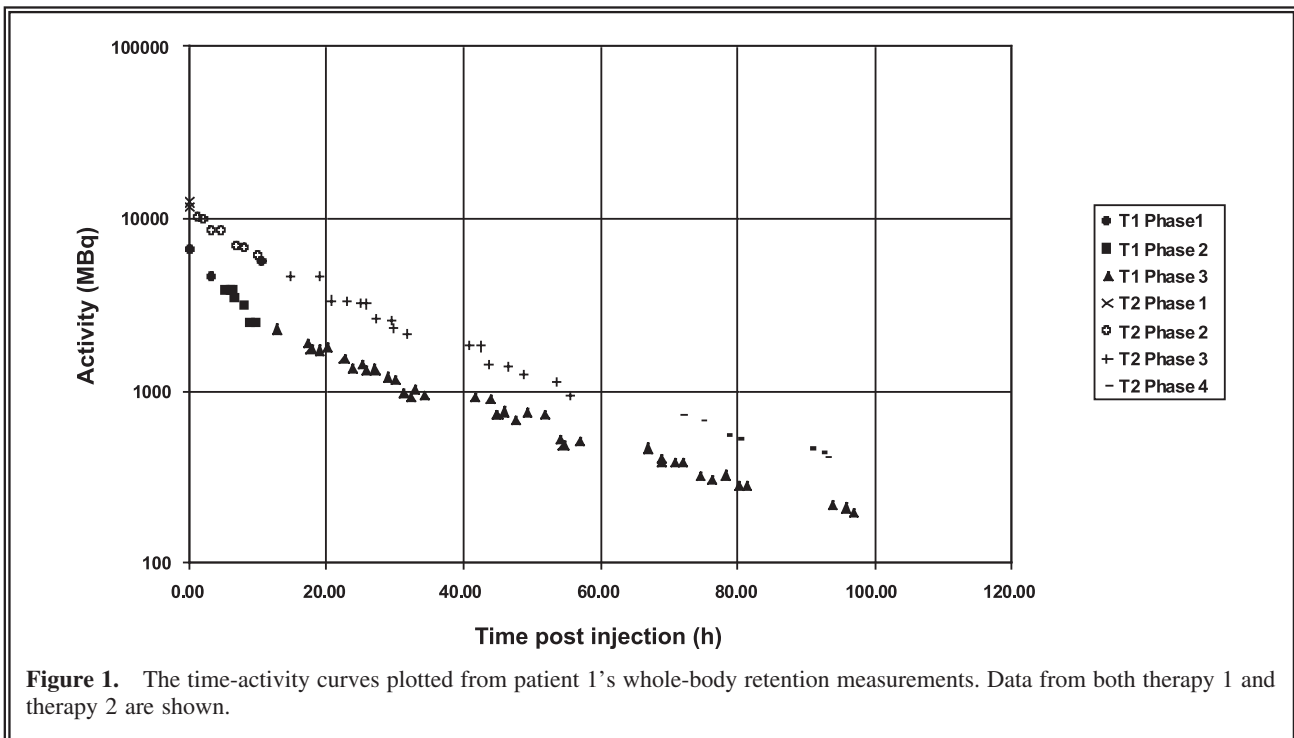
Table 2. Treatment Schedule for ^{131}I -mIBG in 2 Fractions, Given 2 Weeks Apart with Topotecan Followed by Hemopoietic Stem Cell Support

Day	Treatment
0	^{131}I -mIBG course 1: 444 MBq/kg with <i>in vivo</i> whole-body dosimetry.
0-4	topotecan: 0.7 mg/m ² daily.
14	^{131}I -mIBG course 2: to give a combined whole-body absorbed dose of 4 Gy.
14-18	topotecan: 0.7 mg/m ² daily.
24-28	PBSC return.

already been described in detail by Gaze et al.⁷ The activity of the first administration of ^{131}I -mIBG on day 0 was based on the patient's weight (approximately 444 MBq/kg). The activity administered was precisely measured by taking into account any residue in the tubing and vials. This allowed the administered activity to be equated to the first whole-body retention measurement, which was taken immediately after the end of the administration and before the child had voided, using a ceiling-mounted compensated Geiger counter, which was positioned 2 m above the patient's bed. The patient was supine for these measurements, with the bed in its lowest position, so that the geometry was reproducible. Two 1-minute readings were taken at each time point.

Whole-body retention measurements were subsequently taken every 2-4 hours, postvoid, by the nursing staff or comforters and carers. The measurements were continued for the duration of the patient's hospital stay, which ranged from 4 to 8 days, to yield a time-activity curve of between 40 and 70 points (see Fig. 1). From these data, the whole-body radiation dose was calculated using the Medical Internal Radiation Dose (MIRD) schema.⁹ Effective decay phases were user-defined, and the resulting time-activity curve was integrated to determine the cumulated activity, \bar{A} .

The mean absorbed dose, \bar{D} , is given by the product of the cumulated activity and the MIRD S-value. An empirical equation for patient-specific MIRD S-values, based on patient weight,



was generated by interpolating data from the newborn, 1 year old, 5 year old, and adult phantoms¹⁰:

$$S_{(wb \leftarrow wb)} = 1.34 \times 10^{-4} m_p^{-0.921} \text{ Gy MBq}^{-1} \text{ h}^{-1}$$

where m_p is the patient's mass in kilograms.

For the error analysis, the rationale of Flux et al.¹² was assumed, in that within each decay phase, the fractional uncertainties on each data point are identical and that the errors in the time measurements are negligible.

Tumor Dosimetry

The tumor dose was calculated using sequential SPECT scans, acquired either on a Philips Forte (Philips Medical Systems, Milpitas, CA) (patients 1 and 3) or GE Millennium VG gamma camera (GE Healthcare, Waukesha, WI) (patient 2). All of the scans for 1 patient were acquired on the same camera. On both cameras, high-energy general-purpose collimators and a 128×128 matrix were used for the acquisitions. The pixel sizes for the Forte and VG were $0.467 \times 0.467 \text{ cm}^2$ and $0.442 \times 0.442 \text{ cm}^2$, respectively. The number of projections used were 64 on the Forte camera and 72 on the VG. The length of each projection was determined by the activity remaining in the patient. Acquisitions were made with a 20% photopeak energy window centered on 364 keV, with two 6% windows on either side, to allow a triple-energy window scatter correction to be performed during processing.

Prior to patient scanning, dead-time measurements were made on both cameras using a method similar to that described by Bolster.¹¹ Accurately measured activities were added to a phantom situated on the camera face in approximately 100-MBq aliquots to cover a range of 100–2000 MBq. This is equivalent to an uncorrected count rate range of 4500–45,000 cps. At higher count rates, the paralyzable nature of the gamma-camera system makes accurate quantitation impossible. The first scan was, therefore, acquired when the activity remaining in the patient was less than 2000 MBq, as calculated from the whole-body retention measurements. This was between 48 and 70 hours postinjection. To apply the dead-time correction, the mean count rate was calculated from the scatter-corrected single-photon emission computed tomography (SPECT) projections and the associated dead-time factor

applied to the tumor volume of interest (VOI) data. At least three SPECT acquisitions were made for each patient, at 24-hour intervals, following the first scan (excluding weekends).

Each SPECT scan was corrected for scatter using the triple-energy window correction. The scattered counts (C_{scat}) were calculated on a pixel-by-pixel basis, using the following equation:

$$C_{\text{scat}} = 0.5W_{\text{photo}} \times (C_{\text{low}}/W_{\text{low}} + C_{\text{high}}/W_{\text{high}})$$

where C_{low} and C_{high} are the counts acquired in the two windows positioned above and below the photopeak, and W_{photo} , W_{low} , and W_{high} are widths of these windows. Once calculated, C_{scat} is subtracted from the total counts in each pixel to produce the triple-energy window corrected image.

The images were then reconstructed using filtered backprojection with a Butterworth filter of order 5 and a cutoff of 40. A measured uniform attenuation correction, based on the patient outline, was used, with $\mu = 0.11 \text{ cm}^{-1}$. Following the reconstruction, the SPECT scans for each patient were sequentially coregistered.

Two VOIs were chosen to assess the activity in the tumor on each SPECT scan. This was done so that an estimate of the effect of VOI placement on tumor-dose quantitation could be made. VOI 1 was a $3 \times 3 \times 3$ pixel cube centered on the maximum pixel. VOI 2 was a manual outline of the tumor on the coronal slice, containing the maximum pixel on the first scan. This VOI was saved and transferred to data from subsequent days. The number of counts in each VOI was corrected for dead time, length of acquisition, and volume so that the logarithm of VOI counts/cc could be plotted against time postinjection (see Fig. 2). A model of instantaneous uptake, followed by monoexponential decay, was assumed for tumor uptake to allow the effective half-life and the cumulated counts to be calculated.

The cumulative counts were converted to activity using a calibration factor obtained from a calibration phantom acquisition (see Fig. 3). A cylindrical phantom of similar dimensions and functional volume to the tumor was filled with a known concentration of activity and imaged inside a larger (20 cm diameter, 12 cm high) water-filled cylinder, using an identical acquisition and processing protocol to the patient scans. A separate calibration factor was obtained for VOI 1 and VOI 2. A uniform distribution of activity was assumed in both VOIs and a weight-based

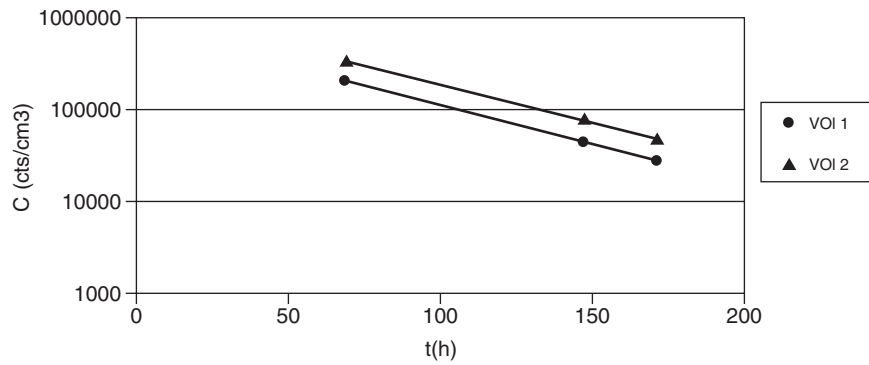


Figure 2. These time-activity curves were generated from patient 2's single-photon emission computed tomography data for therapy 1 using both volume of interest. The monoexponential fits to the data are also shown. The fit for VOI 1 is $C_{VOI1} = 8.55 \times 10^5 e^{-0.02t}$. The fit for VOI 2 is $C_{VOI2} = 1.26 \times 10^6 e^{-0.02t}$.

MIRD S-factor was applied. This was derived using the equilibrium dose constant data from MIRD Pamphlet No. 10¹³ for all ¹³¹I emissions and Stabin and Konijnenberg's absorbed-dose fractions for unit density spheres containing a homogeneous activity distribution.¹⁴ S-factors for 11 tumor masses between 1 and 100 g (1, 2, 4, 6, 8, 10, 20, 40, 60, 80, and 100 g) were calculated and an exponential fit made to the data.

$$S_{\text{tum} \leftarrow \text{tum}} = 3.5 \times 10^{-14} m_t^{-0.977} \text{ Gy Bq}^{-1} \text{ s}^{-1}$$

where m_t is the tumor mass in kilograms.

Tumor-dose ratios (therapy 2 to therapy 1) were calculated to compare the contribution from

each treatment fraction. The error on these ratios was assumed to be the errors in fitting the monoexponential to the plot of VOI counts against time for each therapy added in quadrature, and did not take into account any uncertainties in activity quantification, which were assumed to be the same for each treatment.

RESULTS

The total whole-body doses received by each patient are shown in Figure 4. The total whole-body dose administered was within 9% of the prescribed dose of 4 Gy in all patients. In these 3 patients, prescribing the dose in this manner led to a slight underdosing, as has been previously seen when therapy doses are prescribed from tracer studies.^{11,15} However, there were not enough patients in this preliminary study to assess whether this was a coincidence or a characteristic of this method. The results do show that a dosimetry-guided administration was more accurate than a weight-guided one. For the first therapy, the 3 patients had the same activity administered within $\pm 10\%$, but their whole-body doses ranged from 1.29 ± 0.06 to 2.14 ± 0.08 Gy. Assuming linear extrapolation, if the patients had gone on to receive the same administration for their second therapy, the range of whole-body doses administered would have been 2.58–4.28 Gy instead of the much smaller range of 3.7 ± 0.1 to 3.9 ± 0.3 Gy, which was seen using the dosimetry-guided method.

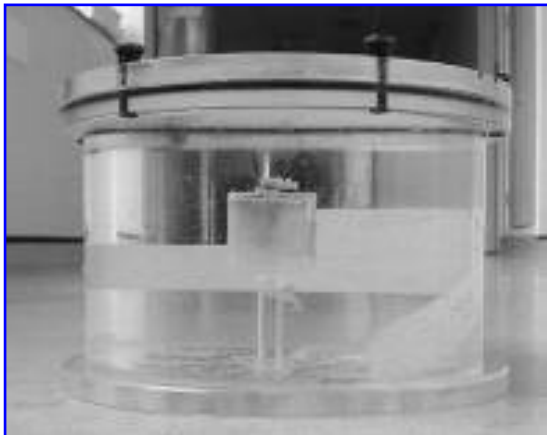


Figure 3. The calibration phantom. A different cylindrical insert was used, depending on the physical dimensions of the patient tumor.

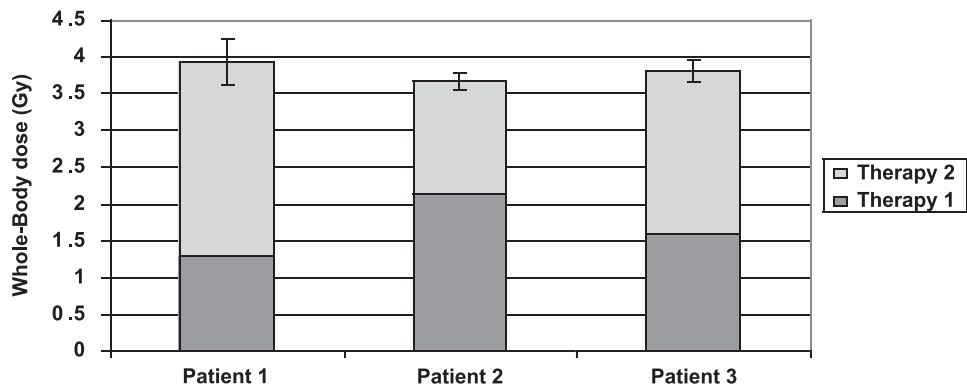


Figure 4. Patient whole-body doses. The planned total dose is 4 Gy. Error bars indicate the uncertainty in the total whole-body dose.

The tumor doses, calculated using our defined protocol, are displayed in Figure 5. Although the data from only 3 patients has been analyzed so far, the huge interpatient variability in absorbed tumor dose received, even when the treatment has been tailored to individual patients according to whole-body dose, is clearly visible. This is owing both to a large variation in initial uptake, and of the effective half-life of ^{131}I -mIBG in the tumor. The initial uptake ranges from 13,300 to 855,000 cts/cc, and the effective half-life from 28.6 to 169 hours. It is also clear that the administration of two courses of treatment allows

for a much higher dose to be given to the tumor than from a single therapy alone.

The error from assuming that ^{131}I -mIBG is taken up instantaneously in the tumor was estimated using both a linear and an exponential model.¹⁶ For the linear model, the effect on cumulative activity was calculated for maximum uptake times of 6, 12, 18, and 24 hours. The exponential model assumes that in the uptake phase, both uptake and clearance are occurring:

$$A_t = A_0 [e^{(-\lambda_1 t)} - e^{(-\lambda_2 t)}]$$

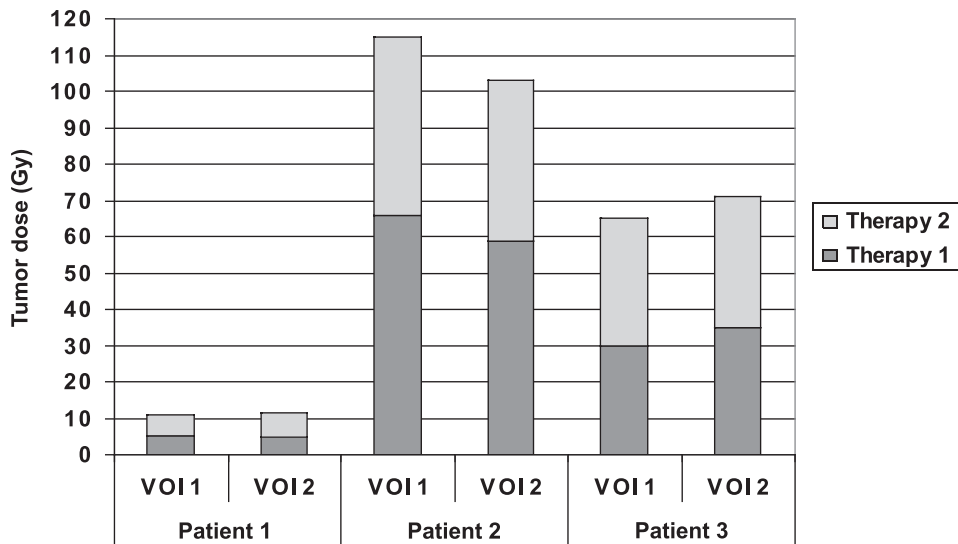


Figure 5. Patient-absorbed tumor doses.

where λ_1 is the decay constant for the effective clearance, λ_2 is the decay constant for the effective uptake, A_t is the activity at time t , and A_0 is the activity at $t = 0$. Time-activity curves were plotted for effective uptake half-lives of 2, 4, 6, 8, and 10 hours. This gave similar curves to those seen with the linear model. Using the longest effective half-life from each model, it was shown that assuming instantaneous uptake can lead to an overestimation in cumulative activity and, therefore, tumor dose of approximately 20%.

The inpatient variation between the two courses of treatment is compared using absorbed-dose ratios in Table 3. The ratio of administered activities and whole-body doses is approximately the same for all patients, thus showing that prescribing the second course of treatment based on the whole-body dose administered by the first should give consistent results. This is also shown in Figure 4. For patient 2, the tumor-absorbed dose ratios are also the same showing that for this patient, the tumor uptake per unit activity is identical for both courses of therapy. For patients 1 and 3, the effective half-life of ^{131}I -mIBG in the tumor is shorter for the second course of therapy. This led to a lower tumor dose per unit activity in the second therapy, which was exacerbated in patient 1 by a lower initial uptake. Although only three sets of patient data have been analyzed, these results show a variation in inpatient response, which needs to be assessed in a larger patient cohort.

DISCUSSION

The whole-body dosimetry data show that using the whole-body retention measurements obtained during treatment 1 to guide the second course of therapy led to a prescribed whole-body dose be-

ing delivered with a greater accuracy than if a weight-based administered activity was used for both treatments. TRT is traditionally administered on an empirical basis, leading to a highly variable whole-body and absorbed-tumor dose. Our initial patient data suggest that administering TRT to a prescribed whole-body dose ensures that a precise whole-body dose would be administered but still would lead to a highly variable dose being absorbed by the tumor.

Ideally, TRT should be prescribed as a dose to the target or as a maximum tolerable dose to normal tissue. Currently, the large number of uncertainties in image quantification means this is not practicable. Absorbed tumor dose ratios provide a simple means of comparing inpatient treatments, which are relatively independent of the dosimetry protocol used.⁸ This can provide useful information on the consistency of patient response to the two treatment fractions, as it allows changes in initial tumor uptake and effective half-life to be monitored without introducing the errors associated with absolute quantification.

Absolute absorbed-dose measurements are necessary to compare interpatient variability for TRT. The accuracy of the tumor dosimetry protocol described in this paper has not yet been assessed but was primarily designed to allow the consistent assessment of tumor doses in a multicenter trial. The errors associated with this tumor dosimetry protocol are currently being evaluated to enable error estimates to be added to Figure 5. The components of the protocol that contributed to the largest source of error will also be identified, so that the procedure can be improved. This will include the assessment of the use of CT-based attenuation correction and anatomical versus functional tumor-volume delineation. Reproducible tumor dosimetry across multiple centers is particularly important in the treatment of neu-

Table 3. Absorbed Tumor-Dose Ratios (T2/T1) for the Two Therapies

	<i>Patient 1</i>	<i>Patient 2</i>	<i>Patient 3</i>
Ratio of administered activity	1.89	0.71	1.36
Ratio of whole-body dose	2.1 ± 0.3	0.71 ± 0.05	1.4 ± 0.1
Absorbed tumor dose ratio VOI 1	1.3 ± 0.4	0.7 ± 0.3	1.0 ± 0.2
Ratio of effective half-life from VOI 1	0.75	1.09	0.75
Absorbed tumor dose ratio VOI 2	1.1 ± 0.3	0.8 ± 0.3	1.2 ± 0.1
Ratio of effective half-life from VOI 2	0.79	1.09	0.73

VOI, volume of interest.

roblastoma with ^{131}I -mIBG, as the small patient numbers make it necessary to use European wide data to build up a significant cohort of patients within a reasonable time frame.

CONCLUSIONS

Initial results indicate that whole-body guided dosimetry allows a whole-body absorbed dose of 4 Gy to be administered by ^{131}I -mIBG to a patient in two consecutive treatments more accurately than empirical dosing. This procedure will now be tested in a larger cohort of patients. The use of absorbed-dose ratios has been shown to provide an accurate method of inpatient treatment comparison, which can now be applied to a larger number of patients to compare levels of tumor uptake and length of effective half-life in repeat treatments. The administration of TRT based on whole-body dosimetry still leads to a wide range of absorbed tumor doses. Therefore, studying the relationship of patient outcome and absorbed tumor dose on a large patient cohort using a consistent protocol is likely to provide invaluable information for improving patient treatment, despite inherent inaccuracies in internal tumor dosimetry. This will hopefully drive the development of an accurate tumor dosimetry protocol to allow the calculation of consistent absorbed tumor doses with a known accuracy and on a routine basis, which should be considered a priority in improving TRT delivery.

ACKNOWLEDGMENTS

This work was supported by a grant from the Neuroblastoma Society, without which such work would not have been possible.

REFERENCES

1. Maris JM, Matthay KK. Molecular biology of neuroblastoma. *J Clin Oncol* 1999;17:2264.
2. Kang TI, Brophy P, Hickeson M, et al. Targeted radiotherapy with submyeloablative doses of ^{131}I -MIBG is effective for disease palliation in highly refractory neuroblastoma. *J Pediatr Hematol Oncol* 2003;25:769.
3. Matthay KK, Villablanca JD, Seeger RC, et al. Treatment of high-risk neuroblastoma with intensive chemotherapy, radiotherapy, autologous bone marrow transplantation, and 13-cis-retinoic acid. *N Engl J Med* 1999;341:1165.
4. Matthay KK, Panina C, Huberty J, et al. Correlation of tumor and whole-body dosimetry with tumor response and toxicity in refractory neuroblastoma with ^{131}I -mIBG. *J Nucl Med* 2001;42:1713.
5. Hoefnagel CA, Voute PA, de Kraker J, et al. Radionuclide diagnosis and therapy of neural crest tumors using iodine-131 metaiodobenzylguanidine. *J Nucl Med* 1987;28:308.
6. McCluskey AG, Boyd M, Ross SC, et al. [^{131}I]metaiodobenzylguanidine and topotecan combination treatment of tumors expressing the noradrenaline transporter. *Clin Cancer Res* 2005;11:7929.
7. Gaze MN, Chang Y, Flux GD, et al. Feasibility of dosimetry-based high-dose 131-metaiodobenzylguanidine with topotecan as a radiosensitizer in children with metastatic neuroblastoma. *Cancer Biother Radiopharm* 2005;20:195.
8. Flux GD, Guy MJ, Papavasileiou P, et al. Absorbed dose ratios for repeated therapy of neuroblastoma with I-131 mIBG. *Cancer Biother Radiopharm* 2003;18:81.
9. Loevinger RL, Budinger TF, Watson EE. *MIRD Primer for Absorbed Dose Calculations*. New York: Society of Nuclear Medicine, 1988.
10. Cristy M, Eckerman K. Specific absorbed fractions of energy at various ages from internal photon sources. In: *ORNL/TM-8381 V1-V7*. Oak Ridge, TN: Oak Ridge National laboratory, 1987.
11. Bolster A. *Report 86: Quality Control of Gamma Camera Systems*. New York: Institute of Physics and Engineering in Medicine, 2003.
12. Flux GD, Guy MJ, Beddows R, et al. Estimation and implications of random errors in whole-body dosimetry for targeted radionuclide therapy. *Phys Med Biol* 2002;47:3211.
13. Medical Internal Radiation Dose committee. *Radionuclide Decay Schemes and Nuclear Parameters for Use in Radiation-Dose Estimation (MIRD Pamphlet 10)*, New York: Society of Nuclear Medicine, 1975.
14. Stabin MG, Konijnenberg MW. Reevaluation of absorbed fractions for photons and electrons in spheres of various sizes. *J Nucl Med* 2000;41:149.
15. Monsieurs M, Brans B, Bacher K, et al. Patient dosimetry for ^{131}I -MIBG therapy for neuroendocrine tumors based on 123-MIBG scans. *Eur J Nucl Med* 2002;29:1581.
16. Liu A, Williams LE, Demidecki AJ, et al. Modelling of tumor uptake to determine time-dose-fractionation effect in radioimmunotherapy. *J Nucl Med* 1994;35:1561.